

A&A manuscript no.  
(will be inserted by hand later)

Your thesaurus codes are:  
07 ( 08.01.1; 08.01.3; 08.05.3; 08.09.2; 08.19.2; 13.21.5)

ASTRONOMY  
AND  
ASTROPHYSICS

# ORFEUS II echelle spectra: On the influence of iron-group line blanketing in the Far-UV spectral range of hot subdwarfs

Jochen L. Deetjen

Institut für Astronomie und Astrophysik, Universität Tübingen, Waldhäuser Str. 64, D-72076 Tübingen, Germany

Received 12 May 2000 / Accepted 14 June 2000

**Abstract.** We present an analysis of the subdwarf O star Feige 67 with a fully metal-line blanketed NLTE model atmosphere based on high-resolution Far-UV (912–2000 Å) and Near-UV (2000–3400 Å) spectra from new ORFEUS II echelle observations and the IUE final archive. The Far-UV spectra are heavily blanketed by iron and nickel lines, preventing the detection of the stellar continuum and complicating the abundance analysis.

Important points concerning the account for blanketing by millions of iron-group lines and for an accurate determination of iron and nickel abundances are discussed: The usage of all theoretically and experimentally known line opacities of the iron-group elements, the consideration of a broad wavelength range for a reliable determination of the stellar continuum flux, and the role of interstellar reddening. This paper outlines a basic approach for spectral analysis of future high-resolution Far-UV spectra of hot compact stars. During this study we re-analyzed the iron and nickel abundance of our exemplary object Feige 67 and confirm their extraordinarily amount.

**Key words:** stars: abundances – stars: atmospheres – stars: evolution – stars: individual: Feige 67 – subdwarfs – Ultraviolet: stars

**Table 1.** Observation log and properties of Feige 67. Photospheric parameters are taken from Haas (1997), except for the Fe and Ni abundances which have been re-analyzed in this paper

Alias	BD+18 2647
$m_V$	12.1
ORFEUS II IDs	5256_1, 5256_2
Observation date	01.12. / 03.12. 1996
Exposure time [s]	2954
IUE LWR IDs (low res.)	03400, 01570, 02944
Observation date	27.05. / 16.11. 1978, 06.01. 1979
Exposure time [s]	240, 480, 597
IUE SWP ID (high res.)	20488
Observation date	20.07. 1983
Exposure time [s]	10 800
$n_{H\ I}$ column density	$(6 \pm 1) \cdot 10^{19} / \text{cm}^2$
Color excess $E_{B-V}$	$0.016 \pm 0.005$
$T_{\text{eff}}$ [K]	$60\,000 \pm 4\,000$
$\log g$ [ $\text{cm/s}^2$ ]	5.0
$n_{\text{He}}/n_{\text{H}}$	$5.3 \cdot 10^{-2}$
$n_{\text{C}}/n_{\text{H}}$	$3.2 \cdot 10^{-5}$
$n_{\text{N}}/n_{\text{H}}$	$1.4 \cdot 10^{-5}$
$n_{\text{O}}/n_{\text{H}}$	$7.3 \cdot 10^{-5}$
$n_{\text{Fe}}/n_{\text{H}}$	$1.4 \cdot 10^{-4}$
$n_{\text{Ni}}/n_{\text{H}}$	$4.2 \cdot 10^{-5}$

## 1. Introduction

With the launch of FUSE in 1999 the window to high-resolution Far-UV spectroscopy has been opened again. In order to prepare an adequate analysis of the upcoming data for hot compact stars, we studied already available high-resolution ORFEUS II echelle spectra using state-of-the-art NLTE (non-local thermodynamic equilibrium) model atmospheres with elaborated model atoms including the opacities of millions of iron and nickel lines.

This paper pursues three aims: First we want to outline a basic approach for spectral analysis of future high-resolution

Far-UV spectra under the viewpoint of iron-group line blanketing. The second aim is a presentation of possible error sources and an estimation of the uncertainties of the abundances derived. The third aim is an improved determination of the iron and nickel abundance of our demonstration object, the sdO Feige 67.

A commonly used approach to determine Fe and Ni abundances is the analysis of individual, prominent line profiles within a narrow wavelength range. For this purpose the observed and the synthetic spectra are normalized to the continuum. However, we will show that the detection of the stellar continuum can be extremely difficult or impossible because of

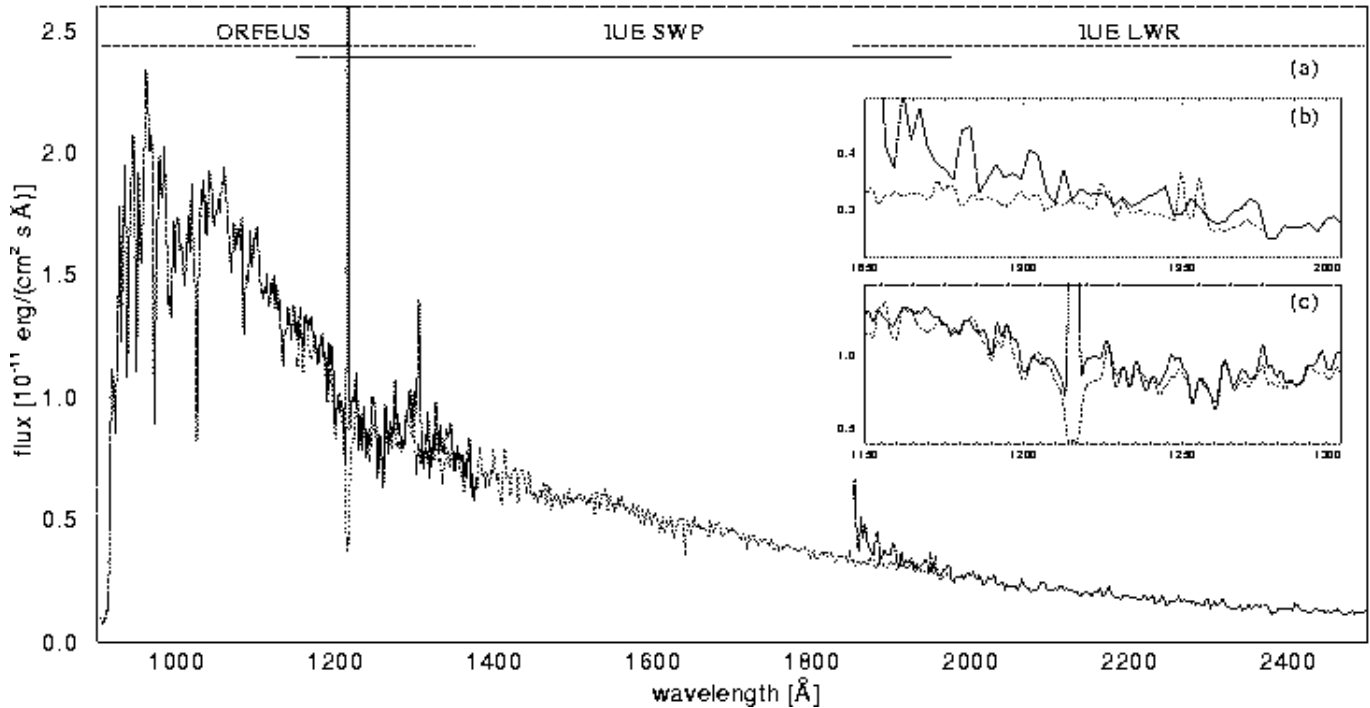


**Fig. 1.** The combined ORFEUS II and IUE spectra of Feige 67. The small inset figures show in more detail the overlap regions of the three spectra, revealing calibration problems at the blue end of the IUE-LWR spectrum. The spectra are smoothed with a Gaussian of FWHM = 2.0 Å

the presence of millions of lines from the iron-group elements. Hence, derived abundances may be afflicted with substantial errors. We will demonstrate that reliable analyses of Far-UV spectra, like from e.g. ORFEUS or FUSE, require a sufficiently large spectral base into the Near-UV region, where line blanketing is less severe, so that the model flux can be normalized to the continuum in that range. For this purpose we analyzed the combined ORFEUS II and IUE spectra of the sdO Feige 67, covering the wavelength range from 900 Å to 3200 Å.

Feige 67 is well suited to demonstrate the difficulties and possible error sources related to the Fe and Ni line blanketing effect, because it is known for its overabundance of the elements (probably due to radiative levitation) and because high-resolution spectra are available and the stellar parameters (see Tab. 1) are well known (Haas 1997; Werner et al. 1998). Haas (1997) derived the effective temperature by the ionization equilibria of Fe and Ni. Our re-analysis of the Fe and Ni abundances results in smaller values compared to the abundances derived by Haas (1997), however, we expect no strong back-reaction on the atmospheric structure which in turn might lead to a different  $T_{\text{eff}}$ . Thus we concentrate here on a thorough analysis of the effect of different Fe and Ni abundances on the synthetic spectrum.

In the following we describe briefly the observation and data reduction (Sect. 2) followed by a short outline of the model atmospheres used (Sect. 3). In Sect. 4 we discuss the four most important steps of the analysis and present the major error sources by means of illustrative figures. The results are summarized in Sect. 5.

## 2. Observations

The echelle spectrometer was one of the focal instruments of the ORFEUS telescope, which was flown on its second mission in November/December 1996. The wavelength range is 900-1400 Å with a spectral resolution of  $\lambda/\Delta\lambda = 10\,000$ . Two separate observations of Feige 67 were obtained with a total integration time of 2954 s (see Tab. 1). The two echelle images were co-added and then the standard extraction procedure was applied (Barnstedt et al. 1999). Feige 67 has been observed with the IUE satellite in the short and in the long wavelength range (see Tab. 1). For our analysis we used the so-called “pre-view spectra” available in the IUE final archive.

Any relative error in the flux calibration of the different instruments with respect to each other will propagate into the error bar of the stellar parameters to be derived, because we will rely on the correct overall shape of the combined spectrum. Fig. 1 shows the good flux calibration of all three observations of Feige 67, because of a good match of the adjoining spectral regions. On hand of our final model we show in Fig. 2 the strong line blanketing in the Far-UV spectral region, which results in an overall flux depression, particularly in the degraded spectrum.

## 3. NLTE Model atmospheres

Based on the results of Haas (1997) we calculated a plane-parallel non-LTE model atmosphere with  $T_{\text{eff}} = 60\,000$  and  $\log g = 5.0$  in radiative and hydrostatic equilibrium. According to Haas (1997) the Fe and Ni abundances were set to 10 and 70

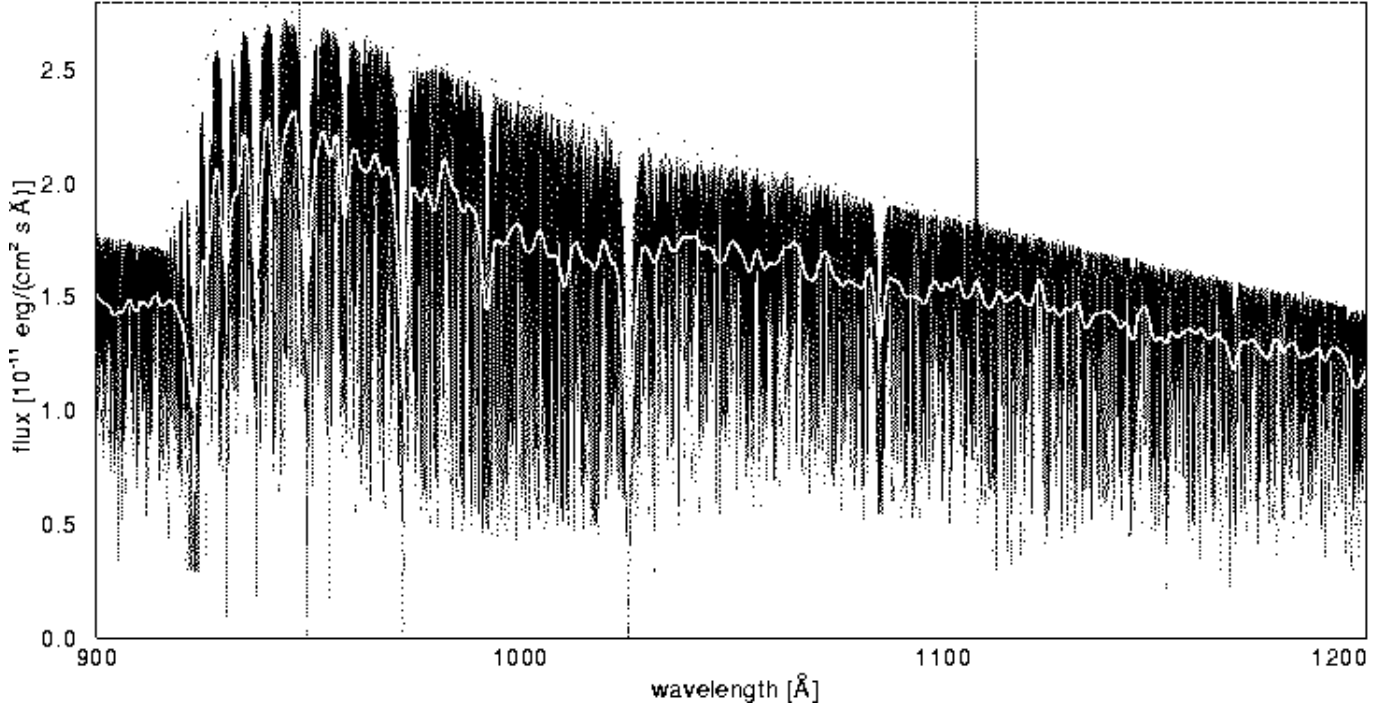


**Fig. 2.** Synthetic spectrum of the final model (including interstellar Lyman line absorption) for Feige 67, demonstrating the high density of Fe and Ni lines. Overplotted (white line) is the same spectrum, but degraded with a Gaussian of  $\text{FWHM} = 2.0 \text{ \AA}$ , matching the smoothing of the observations shown in Fig. 1. The dash-dotted line indicates the continuum model flux. Model parameters are given in Tab. 1

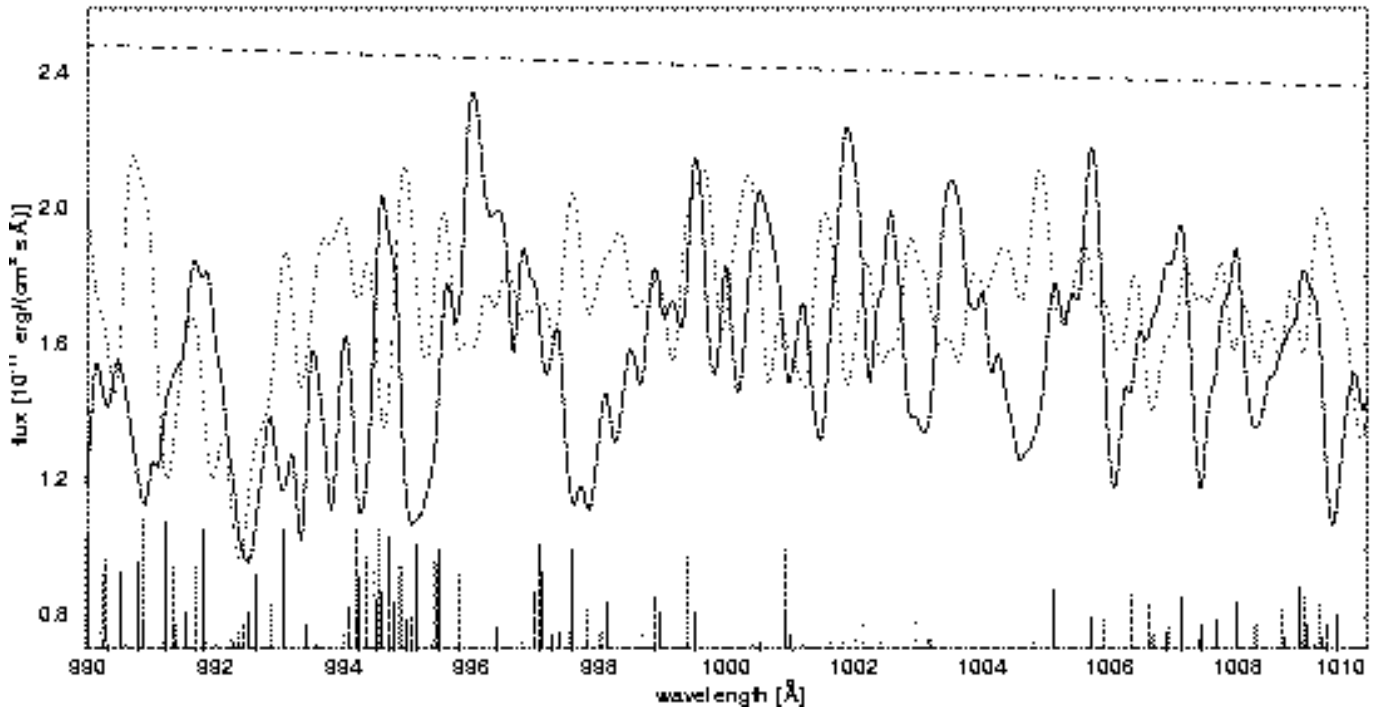


**Fig. 3.** Detail of the ORFEUS II spectrum (thick line) with the final model (thin line). The flux level, which falls well below the continuum (dash-dotted line) is matched satisfactorily, however, the identification of individual lines is not possible because of inaccurate line positions in the full Kurucz line list. Vertical lines at the bottom panel mark Ni/Fe lines in the model with  $\text{gf-values} \geq -2.0$  (bar length proportional to  $\log \text{gf}$ ). The spectra are smoothed with a Gaussian of  $\text{FWHM} = 0.25 \text{ \AA}$

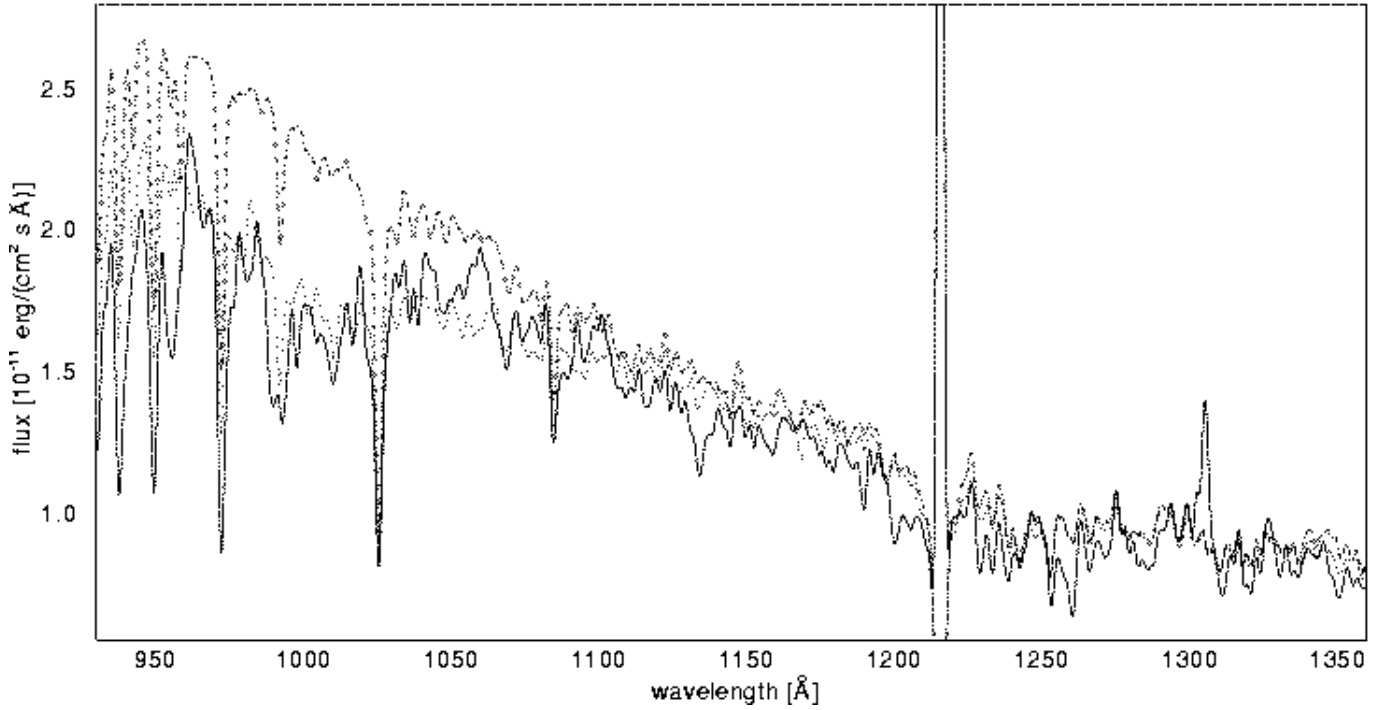


**Fig. 4.** ORFEUS II spectrum (thick line) compared to two model spectra (including reddening and H I absorption) which are calculated with the full Kurucz line list in one case (thin line) and the small subset of experimentally known lines in the other case (thin line with circles). The full list is necessary to reproduce the spectral shape particularly below 1100 Å. All spectra are smoothed with a Gaussian of FWHM = 2.0 Å

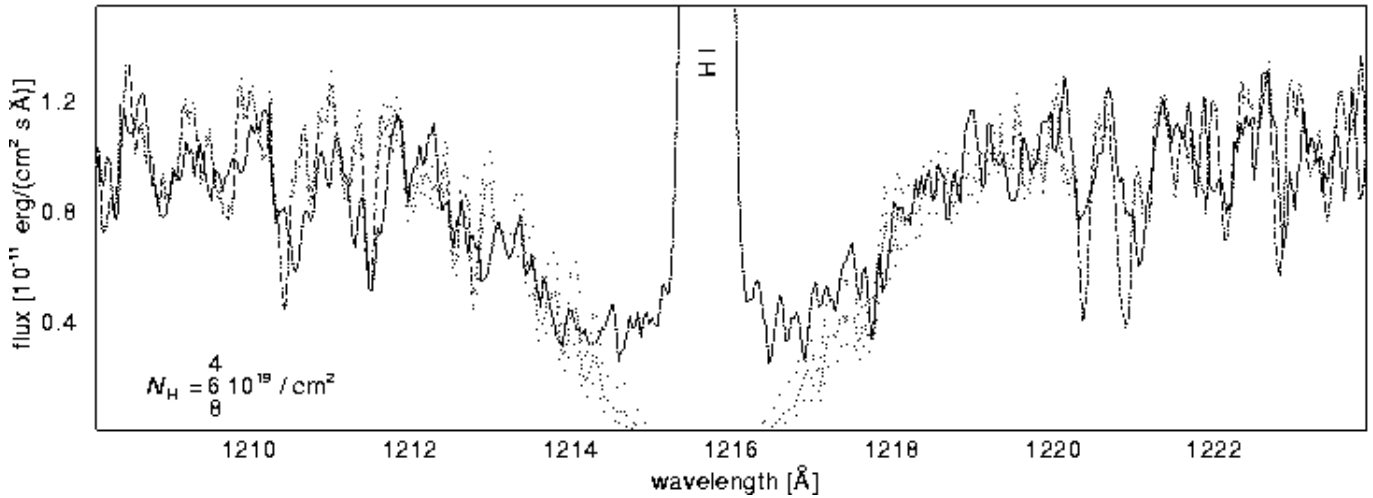


**Fig. 5.** The interstellar H I column density is derived from this fit to the Ly $\alpha$  profile in the ORFEUS II spectrum. The spectra are smoothed with a Savitzky-Golay filter (observation:  $M=4$ ,  $n_L+n_R+1=9$ ; model:  $M=4$ ,  $n_L+n_R+1=17$ )

times solar, respectively. In order to calculate synthetic spectra with different Fe and Ni abundances, a single formal solution of the radiation transfer equation is performed keeping fixed the whole model structure.

The computer code is based on the Accelerated Lambda Iteration method (Werner & Husfeld 1985; Werner 1986) and it can handle the line blanketing of iron-group elements by a statistical approach using superlevels and superlines with an

opacity sampling technique (Anderson 1985; Werner & Dreizler 1999) as described in Deetjen et al. (1999).

A summary of the detailed model atoms used is given in Tab. 2. Test calculations for Feige 67 have shown, that Fe V and Fe VI are the dominant ionization stages in those atmospheric layers where the iron lines are formed.

For the calculation of opacities of iron group elements one can choose between a subset of the Kurucz (Kurucz 1991) line list, containing only lines known from laboratory spec-

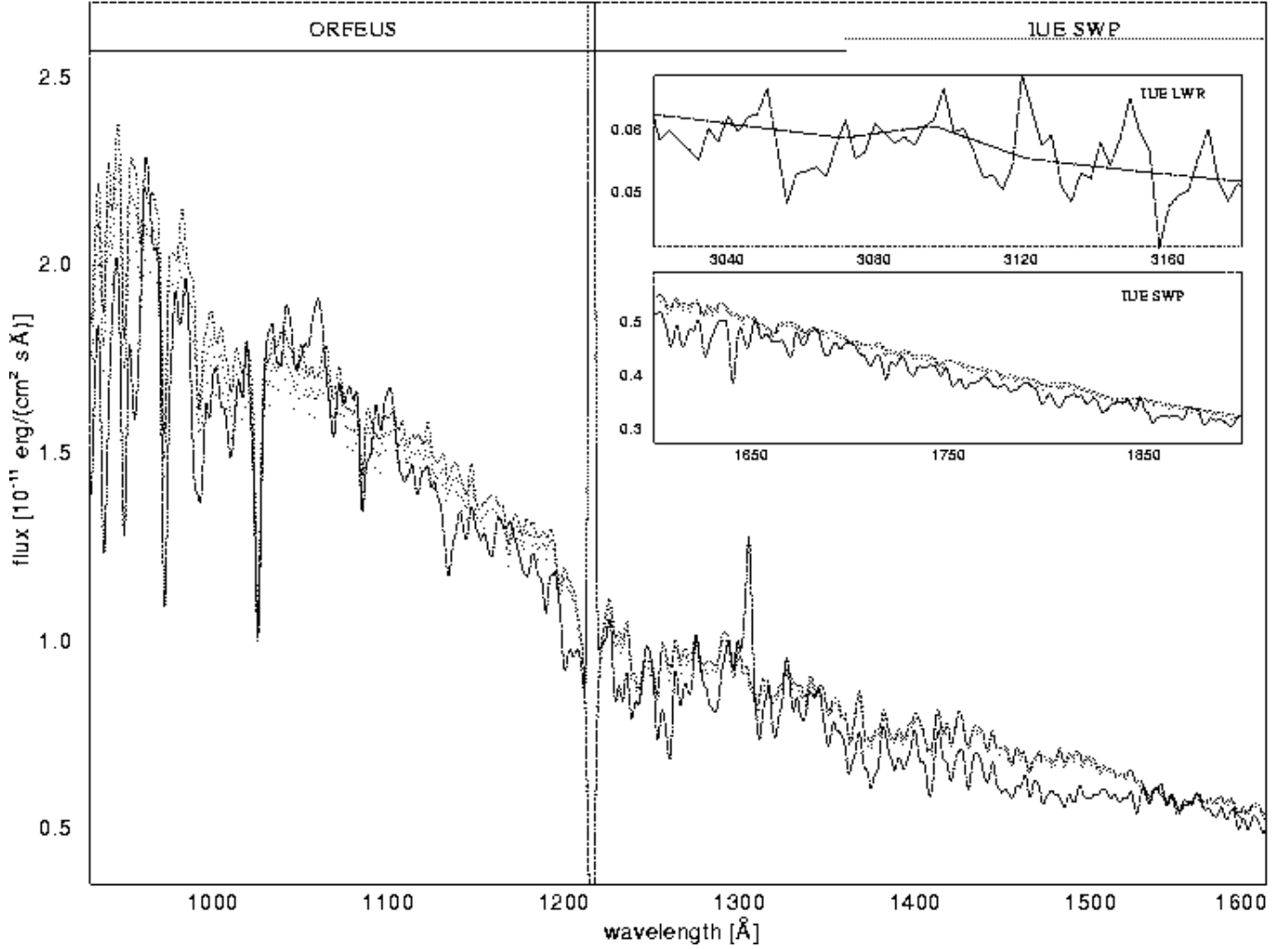


**Fig. 6.** ORFEUS II spectrum (thick line) compared to the final model which is not attenuated by the interstellar extinction (thin dash-dotted line) and to final model which is attenuated by interstellar extinction for two values of  $E(B-V)$ , representing the error margin ( $E(B-V)=0.011$  and  $0.021$ ). The inset figures show the IUE spectra for comparison. The spectra are smoothed with a Gaussian of  $\text{FWHM} = 2.0 \text{ \AA}$  and the reddened models are normalized to the observation near  $3000 \text{ \AA}$

tra, and the full one, augmented by a vast number of theoretically computed lines. The full line list is afflicted with uncertainties in oscillator strengths and wavelength positions, preventing the identification of individual lines when comparing with observed spectra (see Fig. 3). The small list on the other hand causes much too less total opacity. Fig. 4 demonstrates the high relevance of using the full line list for further analysis in the Far-UV range. It also demonstrates the impossibility to determine the stellar continuum, so that analyses with model atmospheres must rely on a correct flux normalization in the Near-UV where line blanketing is less severe.

#### 4. Analysis

In the following we discuss and determine the most important parameters which influence the observed spectrum. Due to their interacting character the analysis has to be done iteratively.

##### 4.1. $H\text{I}$ column density

The interstellar  $H\text{I}$  column density along the line of sight is derived from the  $\text{Ly}\alpha$  profile in the ORFEUS II spectrum (Fig. 5). We applied different models and found no dependency of the derived column density on the adopted Fe and Ni abundance (which might be caused by strong blending of the  $\text{Ly}\alpha$  profile) and obtained  $N_{H\text{I}} = (6 \pm 1) \cdot 10^{19} / \text{cm}^2$ . The same result has been derived from the  $\text{Ly}\alpha$  profile in the IUE-SWP spectrum. Note that we did not try to normalize the model continuum to a putative local stellar continuum near  $\text{Ly}\alpha$ , instead we relied on the flux normalization in the Near-UV (see below). Therefore interstellar reddening has to be accounted for, otherwise one underestimates  $N_{H\text{I}}$  by approximately 0.1 dex. This in turn (as reddening is calculated from  $N_{H\text{I}}$ ) would cause an overestimation of the iron-group abundance by about a factor two.

Another source of error can be too strong smoothing of the observation or the model. Even convolution with a Gaussian of

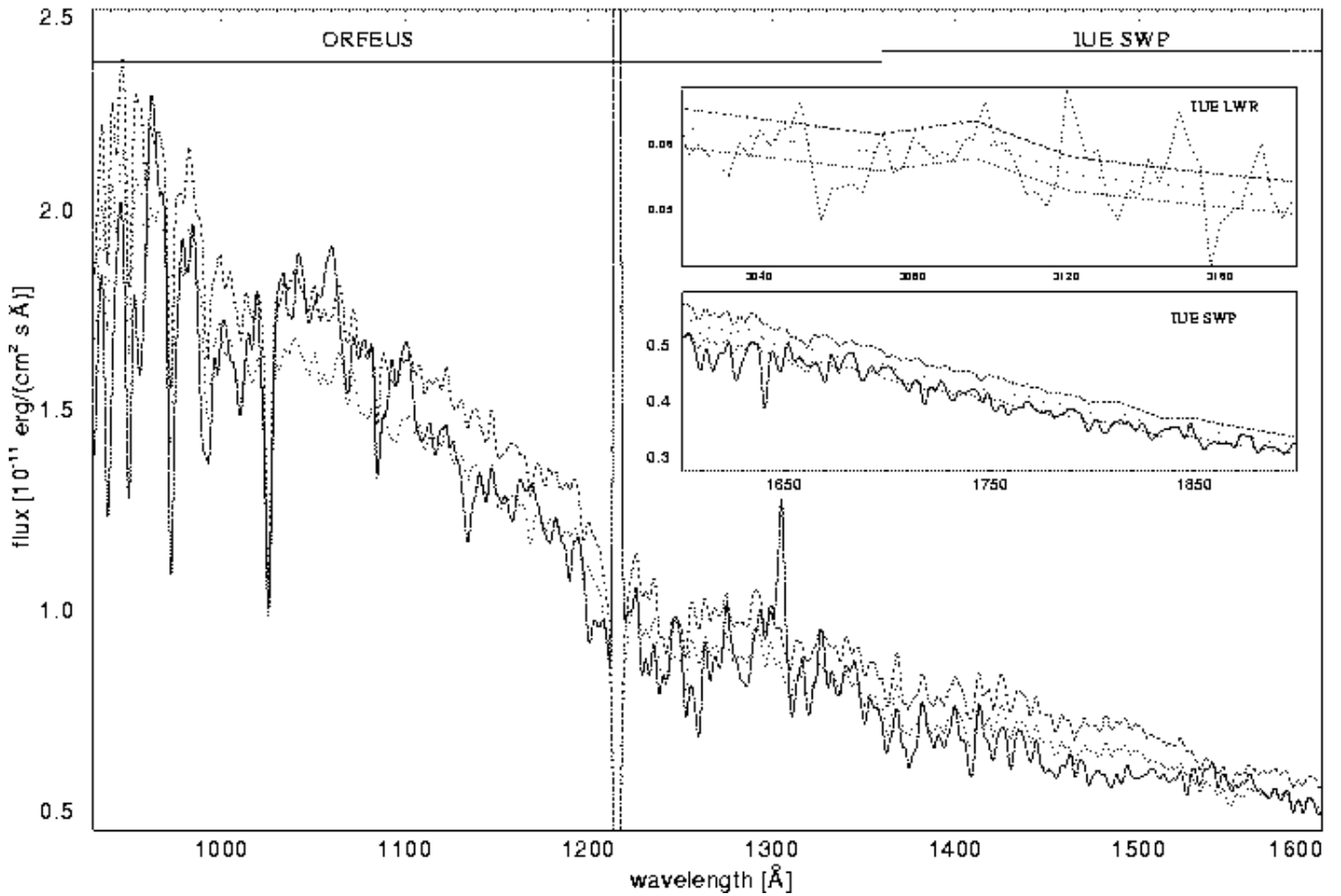


**Fig. 7.** The synthetic spectrum is normalized to the observation (thick line) near  $\lambda = 3000 \text{ \AA}$  to avoid the strong line blanketing in the Far-UV. The two thin lines denote the normalized model spectrum with the normalization factor varied by  $\pm 5\%$ , representing the uncertainty in normalization. The two inset figures show details from the IUE spectra with the best fit model (thin dashed-dotted line) plotted additionally. All spectra are smoothed with a Gaussian of  $\text{FWHM} = 3.0 \text{ \AA}$

only  $\text{FWHM} = 0.2 \text{ \AA}$  corrupts the interstellar  $\text{Ly}\alpha$  profile because of many blending iron group lines. Therefore we used a low-pass filter for noise-reduction, the Savitzky-Golay smoothing filter, as described in Press et al. (1995).

#### 4.2. Interstellar reddening

Based on the determined column density, the color excess can be calculated to  $E_{(B-V)} = 0.016 \pm 0.005$ , using the formula of Groenewegen & Lamers (1989)

$$N_{\text{HI}} = (3.8 \pm 0.9) \times 10^{21} E_{(B-V)}.$$

An independent determination of the color excess could not be realized, because it is too small to produce a detectable  $2200 \text{ \AA}$  feature in the IUE-LWR spectrum.

In the literature the applicability of the above formula is debated as well as the choice of the interstellar extinction law itself. Hence some authors try to determine such a law adapted to their specific observation. Generally, however, this is impossible, so that in our case we expect a systematic error of at least 0.1 dex (using the interstellar extinction law as described

in Seaton (1979)) in addition to the statistical error, which is estimated to 0.1 dex from Fig. 6. It is clear that the neglect of interstellar reddening in the Far-UV range results in an underestimation of the stellar flux level. This would lead to an overestimation of the Fe and Ni abundances, by about a factor of 1.0 dex in our specific case.

#### 4.3. Normalization of the model to the observation

As already mentioned above, strong line blanketing in the Far-UV requires a model flux normalization in the Near-UV, where reduced blanketing does not prevent detection of the stellar continuum. We determined the position of the continuum at the red end of the spectrum above  $3000 \text{ \AA}$ . In Fig. 7 the resulting synthetic flux has been multiplied by a factor of 0.95 and 1.05, respectively, representing the uncertainty of fixing the continuum in the Near-UV. A determination of the continuum only within the Far-UV range results in an analytical uncertainty in the iron and nickel abundance of about a factor two (compare Fig. 7 with 8). Neglecting the general slope of the spectrum in

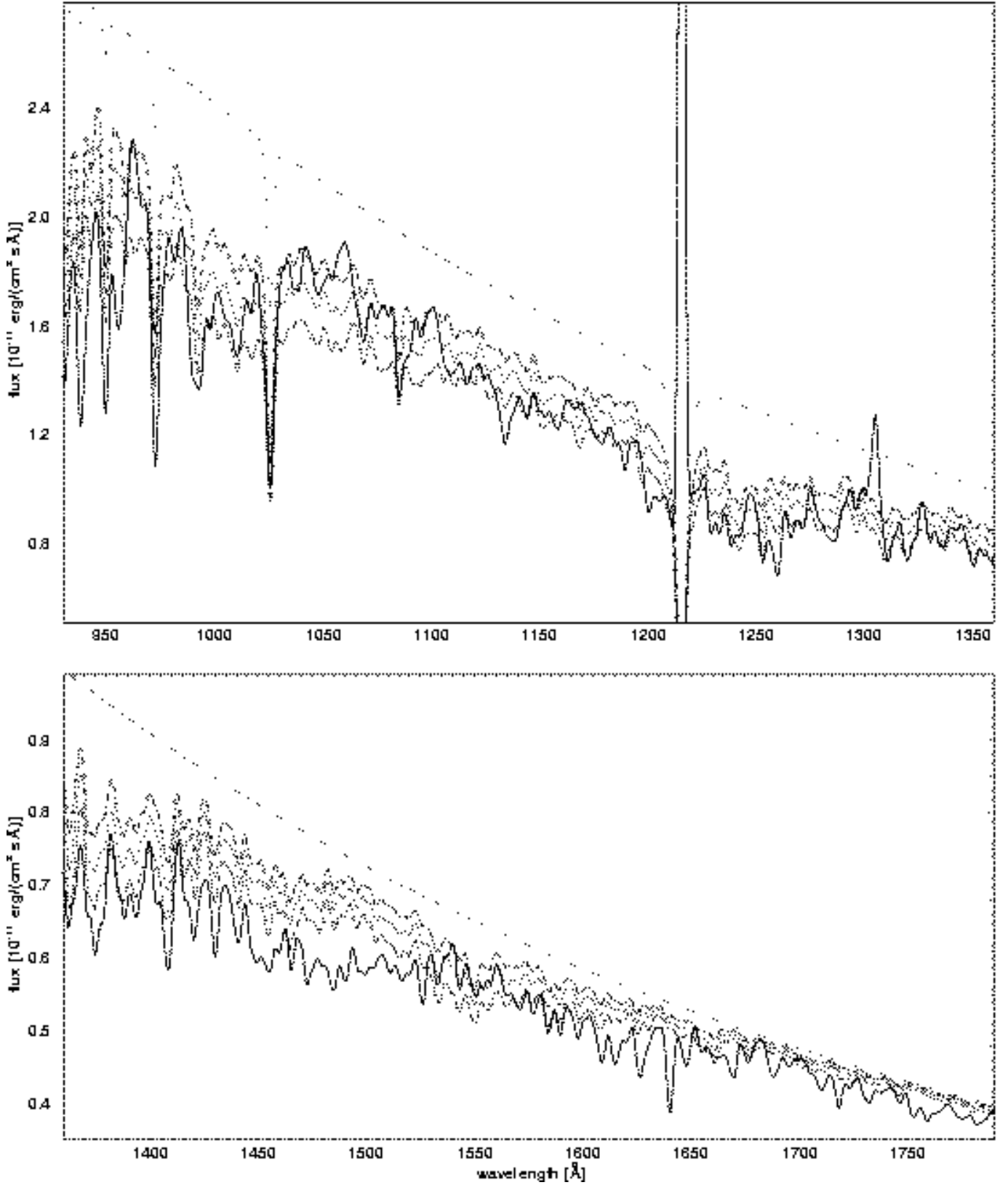


**Fig. 8.** Detailed comparison of the final model (thin line) to the ORFEUS II (top panel) and IUE-SWP (bottom panel) spectra (thick lines). The other two thin lines represent models with Fe and Ni abundances varied by a factor two, representing the analysis error. Between 1500 Å and 1600 Å all models overestimate the stellar flux, perhaps due to missing opacity from other iron group elements which are disregarded in this study. The dashed-dotted line denotes the model continuum. All spectra smoothed with a Gaussian of FWHM = 3.0 Å

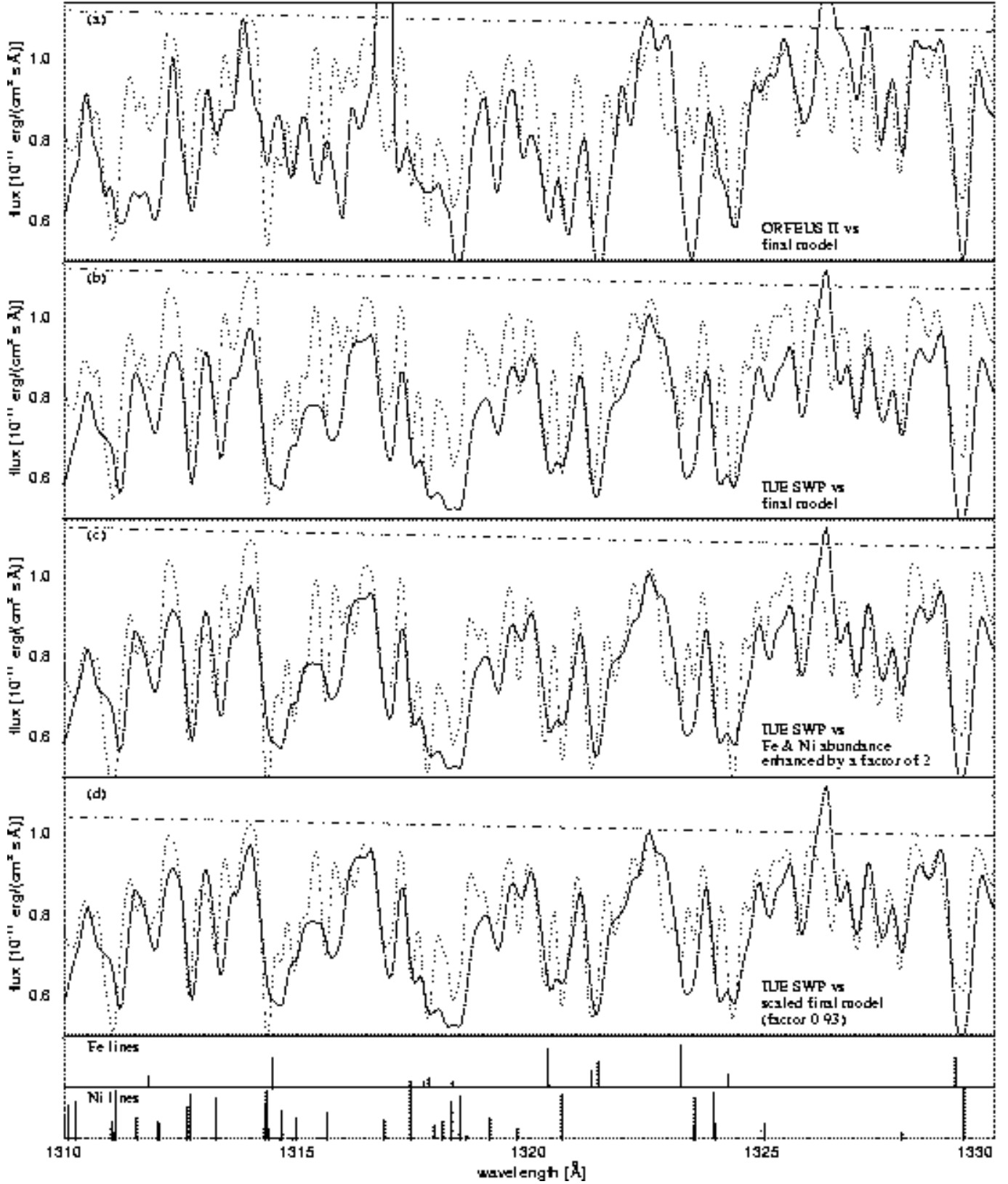


**Fig. 9.** Detail of another UV wavelength region of Feige 67, where IUE and ORFEUS II spectra overlap, showing observed spectra (thick line) and final model spectra (thin line). The dashed-dotted line represents the model continuum. Panel (a): ORFEUS II vs. final model. Panel (b): IUE-SWP vs. final model. Panel (c): IUE-SWP vs. model with Fe and Ni abundances enhanced by a factor two. Panel (d): IUE vs. scaled model (factor 0.93). All spectra are smoothed with a Gaussian of FWHM = 0.2 Å



**Table 2.** Summary of model atoms used in our model atmosphere calculations. Numbers in brackets denote individual levels and lines used in the statistical NLTE line blanketing approach for iron and nickel. The model atom for each chemical element is closed by a single level representing the highest ionization stage (not listed explicitly)

element	ion	NLTE levels	lines
H	I	16	56
He	I	29	91
	II	32	115
C	III	58	231
	IV	57	201
N	III	1	0
	IV	90	368
	V	36	98
O	IV	30	99
	V	44	86
	VI	52	237
Fe	IV	7 (6 472)	25 (1 027 793)
	V	7 (6 179)	25 (793 718)
	VI	8 (3 137)	33 (340 132)
	VII	9 (1 195)	39 (86 504)
	VIII	7 (310)	27 (8 724)
Ni	IV	7 (5 514)	25 (949 506)
	V	7 (5 960)	22 (1 006 189)
	VI	7 (9 988)	22 (1 110 584)
	VII	7 (6 686)	18 (688 355)
	VIII	7 (3 600)	27 (553 549)
total		525 (49 041)	1845 (6 565 054)

the Near-UV and the Far-UV may result an additional systematic error of the same magnitude.

#### 4.4. Variation of the iron and nickel abundance

After the preparatory steps discussed above one is now in the position to determine the abundances of Fe and Ni by fitting the spectral slope. Fig. 8 demonstrates the sensitivity of the flux distribution against the simultaneous variation of the Fe and Ni abundances in the model by  $\pm 0.3$  dex. Detailed calculations have shown, that modifications in the Fe abundance are mainly noticeable in the ranges 960–1140 Å and 1360–1510 Å, whereas modifications in the Ni abundance occur dominantly in the range 1030–1330 Å. The resulting abundances of the best fitting model are given in Tab. 1.

A determination of the Fe and Ni abundance by fitting the profile of individual lines (Fig. 9) is rather problematic because of, as stated above, blending by lines with inaccurately known wavelength positions and oscillator strengths.

## 5. Conclusion

In order to derive the iron and nickel abundances in the sdO star Feige 67 we proceeded in two major steps. At first we considered the shape of the spectrum over a broad wavelength range. Here we focused on the correct consideration of all effects of physical relevance, i.e. large model atoms,  $n_{\text{H I}}$  determination, and interstellar reddening as well as on effects of technical relevance, i.e. determination of the continuum and quality of the flux calibration. As a result we could demonstrate the important influence of these details for the second step, where the Fe and Ni abundances are derived from the ORFEUS II spectrum.

We confirmed the high Fe and Ni abundances of Feige 67 and find 3.5 and 26.5 times solar, respectively (see Tab. 1), which are however a factor three smaller than the results by Haas (1997). Becker & Butler (1995a,b,c) derived Fe and Ni abundances of approximately 10 times solar, based on the IUE-SWP observations and using models with  $T_{\text{eff}}=70\,000$  K. The reasons for this more deviating result can be i) the lower, probably more realistic  $T_{\text{eff}}$  of our model (based on the analysis of Haas (1997)), ii) our use of self-consistent metal-line blanketed models in contrast to the Becker & Butler approach, and iii) an increased accuracy of our analysis using combined ORFEUS II, IUE-SWP and IUE-LWR observations.

At present the accuracy of Fe and Ni abundance determinations is limited mainly by uncertainties of the atomic data available and by the S/N ratio and resolution of the spectra. Therefore an error in the derived abundances of a factor of about two has to be accepted. For a reliable analysis of Far-UV spectra complementary Near-UV observations are recommended. Uncertainties in the knowledge of interstellar reddening enlarges the systematic error.

Generally, we have demonstrated the importance of correctly considering iron-group line blanketing for the analysis of future high-resolution Far-UV spectra of hot compact stars. This more detailed analysis technique enables to fully benefit from the improved high-resolution spectra of FUSE.

*Acknowledgements.* We would like to thank Stefan Dreizler, Stefan Haas, Thomas Rauch, and Klaus Werner for many helpful discussions and careful reading of the manuscript. This work is supported by the Deutsches Zentrum für Luft- und Raumfahrt (DLR) under grant 50 QV 97054. The IUE data presented in this paper were obtained from the Multimission Archive at the Space Telescope Science Institute (MAST).

## References

- Anderson L.S., 1985, ApJ 298, 848
- Barnstedt J., Kappelman N., Appenzeller I., et al., 1999, A&AS 134, 561
- Becker S.R., Butler K., 1995a, A&A 294, 215
- Becker S.R., Butler K., 1995b, A&A 301, 187
- Becker S.R., Butler K., 1995c, A&A 300, 453
- Deetjen J.L., Dreizler S., Rauch T., Werner K., 1999, A&A 348, 940
- Groenewegen M.A.T., Lamers H.J.G.M., 1989, A&AS 79, 359

- Haas S., 1997, Dissertation, Universität Erlangen-Nürnberg
- Kurucz R.L., 1991, In: Crivellari L., Hubeny I., Hummer D.G. (eds.) *Stellar Atmospheres: Beyond Classical Models*. NATO ASI Ser. C 341, Kluwer, Dordrecht, p.441
- Press W.H., Teukolsky S.A., Vetterling W.T., Flannery B.P., 1995, *Numerical Recipes in C, The Art of Scientific Computing*, Cambridge Univ. Press, Cambridge, New York, Port Chester, Melbourne, Sydney, 2<sup>nd</sup> edition
- Seaton M.J., 1979, MNRAS 187, 73
- Werner K., 1986, A&A 161, 177
- Werner K., Dreizler S., 1999, J. Comp. Appl. Math. 109, 65
- Werner K., Dreizler S., Haas S., Heber U., 1998, In: Wamsteker W., Riestra R.G. (eds.) SP-413 "Ultraviolet Astrophysics, Beyond the IUE Final Archive", ESA, p.301
- Werner K., Husfeld D., 1985, A&A 148, 417